ChemComm

Cite this: *Chem. Commun.*, 2012, **48**, 597–599

www.rsc.org/chemcomm

COMMUNICATION

In situ spontaneous reduction synthesis of spherical Pd@Cys-C_{60} nanoparticles and its application in nonenzymatic glucose biosensors†

Xia Zhong, Ruo Yuan* and Yaqin Chai

Received 30th September 2011, Accepted 10th November 2011
DOI: 10.1039/c1cc16081h

Novel spherical Pd@Cys-C_{60} nanoparticles were synthesized using an *in situ* spontaneous reduction process without any other reducing agent. A nonenzymatic electrochemical biosensor was developed for the detection of glucose based on the spherical nanoparticles film.

Despite the increasing interest from the scientific community in carbon nanotubes and graphene, fullerene (C_{60}) still plays an important role in the family of nanocarbons.[1,2] C_{60}, a third allotrope of carbon, is a hollow carbon sphere that has been investigated extensively since 1985.[3,4] C_{60} is still found attractive by researchers because of its remarkable physical and chemical properties, which prompt such materials to have potential applications in several fields, ranging from sensors and photovoltaic cells to nanostructure devices for advanced electronic applications.[5,6] The spherical fullerenes not only accelerate electron transfer and charge shift, but also slow down charge recombination. Due to the notable electrochemical properties, C_{60} as a novel mediator has been applied to determine dopamine.[7]

However, C_{60} has relatively poor water solubility, which limits its application in biology.[2] Recently, various stable, well-characterized, highly soluble and biocompatible C_{60} derivatives have been designed and synthesized. As a result, they further accelerate and broaden the application of C_{60}-based fullerenes.[6] Originally, the surfactants such as cyclodextrin[8] and polyethylene glycol[9] were used to improve the solubility. Later, the surface of C_{60} was decorated with many multi-polar groups (such as amido, hydroxyl and carboxyl) to produce water-soluble compounds.[10–14] C_{60}, with rich conjugated π electrons, can react with amines.[15,16] L-Cysteine (Cys) is an α-amino acid, containing $-NH_2$ groups. It is conceivable that Cys can be alternative for chemical functionization of C_{60} to improve C_{60} water solubility.

It is implicated that C_{60} shows somehow affinity characteristics of metal on the basis of its distorted structure.[17–19] Due to the unique affinity to metal, C_{60}-Pt nanoparticles were prepared and immobilized on a gold electrode which have exhibited remarkable methanol oxidation activity.[17,20] It has also been reported that the electrodes modified with C_{60}-based materials act as excellent working electrodes owing to their high electroactive surface area, excellent electronic conductivity as well as good biocompatibility.[21] It is well known that palladium nanoparticles (PdNPS) are one of the most efficient catalysts. PdNPS-based biosensors have been reported for glucose and effectively improved sensitivity and selectivity towards the oxidation of glucose.[22] Synthesizing water-soluble C_{60} hybrid materials with palladium and studying their physical, chemical and photoelectronic properties are very important for exploring C_{60}-based new materials.[23]

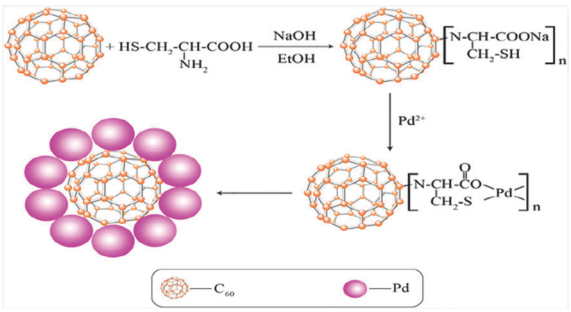

Scheme 1 Typical synthetic process of Pd@Cys-C_{60} nanoparticles.

In this work, a two-step strategy was employed to synthesize novel spherical Pd@Cys-C_{60} nanoparticles *via* an *in situ* spontaneous reduction process (Scheme 1). First, C_{60} was functionalized with Cys to improve its biocompatibility and hydrophilicity. Second, the water-soluble Cys-C_{60} derivative was assembled with Pd^{2+} to form the coordination compound of Pd^{2+}(Cys-C_{60})$_n$, and then the spherical Pd@Cys-C_{60} nanoparticles were formed by the *in situ* spontaneous reduction process without any other reducing agent. Finally, the resulting product was obtained by filtration, washing, and drying at 50 °C under vacuum.

The transmission electron microscopy (TEM) images of the products obtained by each step are shown in Fig. 1. A nearly transparent C_{60} was exhibited with particle diameter about 5 to 10 nm (Fig. 1A).[24] Fig. 1B illustrates that the cross-linking Cys-C_{60} derivatives had been formed. As show in Fig. 1C, the dendritic coordination compounds of Pd^{2+}(Cys-C_{60})$_n$ were synthesized by Pd^{2+} coordination interaction with –COOH

Key Laboratory on luminescence and real-timeanalysis, ministry of education, College of Chemistry and Chemical Engineering, Southwest University, Chongqing 400715, PR China. E-mail: yuanruo@swu.edu.cn; Fax: +86 23 68254000; Tel: +86 23 68252277

† Electronic supplementary information (ESI) available. See DOI: 10.1039/c1cc16081h

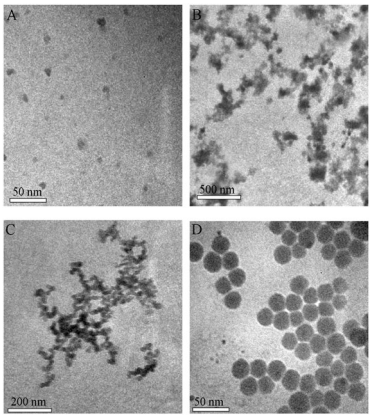

Fig. 1 TEM photos of (A) C_{60}, (B) Cys-C_{60} derivatives, (C) Pd^{2+}(Cys-C_{60})$_n$ and (D) Pd@Cys-C_{60}.

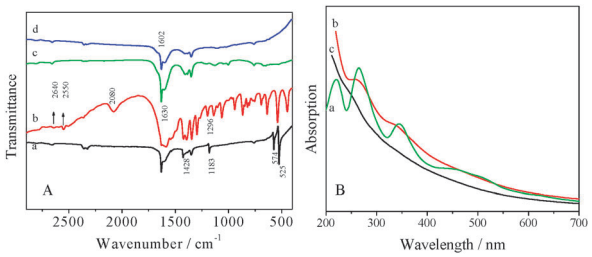

Fig. 2 (A) FT-IR spectra of the (a) C_{60}, (b) Cys, (c) Cys-C_{60} derivatives and (d) Pd@Cys-C_{60}; (B) UV-Vis spectra of (a) C_{60}, (b) Cys-C_{60} derivatives and (c) Pd@Cys-C_{60}.

and –SH of Cys. The TEM image shown in Fig. 1D confirms that we have synthesized spherical Pd@Cys-C_{60} nanoparticles with an average size of around 25 nm. The Pd@Cys-C_{60} nanoparticles were formed *via in situ* spontaneous reduction of Pd^{2+}(Cys-C_{60})$_n$ without any other reducing agent. The possible explanation is that the Pd^{2+} is reduced Pd by the synergetic effect of Cys and C_{60}.[25]

The observation by FT-IR and UV-Vis further supports the Cys-C_{60} and Pd@Cys-C_{60} nanoparticles (Fig. 2). In the FT-IR shown in Fig. 2A, there are four characteristic bands at 525, 574, 1183 and 1428 cm^{-1} (curve a), which consistently matched the typical four dipole-allowed of C_{60}.[17] Comparing with the spectra of Cys (curve b) and Cys-C_{60} (curve c), the most important difference between them is that the characteristic peaks of –NH_3^+ at 2080 and 2640 cm^{-1} disappeared in curve c. This result can be explained by the covalent reaction of –NH_2 to C_{60}. Interestingly, a stretching vibration peak of –SH at 2550 cm^{-1} was shown in curve b not in curve d. Furthermore, the stretching vibration of C═O in Cys-C_{60} at 1630 cm^{-1} is largely decreased by 28 cm^{-1} in Pd@Cys-C_{60}. In the end, the wagging vibration peak at 1296 cm^{-1} represents CH_2–S from Cys, however, the peak shifted to 1205 cm^{-1} in a Cys-C_{60} product and it was totally missed in Pd@Cys-C_{60}.

UV-Vis absorption spectroscopy was further used to characterize the component obtained by each step. As shown in Fig. 2B, three strong optical absorption peaks belonged to the dipole-allowed transitions in pristine C_{60} are also observed at 221, 265, and 345 nm (curve a), respectively, which is in line with other reported results.[26] After Cys-C_{60} derivatives were

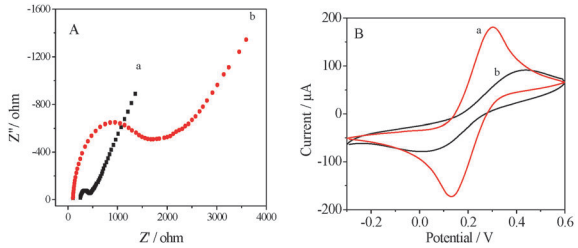

Fig. 3 EIS (A) and CVs (B) of the electrodes at different stages: (a) bare GCE, and (b) Pd@Cys-C_{60}/GCE.

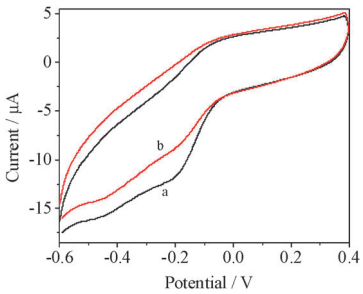

Fig. 4 CVs of the proposed electrode without (a) glucose, with (b) 0.5 mM glucose in 0.1 M PBS (pH 7.4), scan rate: 100 mV s^{-1}.

formed, the absorption shows a red-shift trend of the surface-plasmon band (curve b). The characteristic absorbance peak is missing when Pd@Cys-C_{60} was synthesized which suggested that the Pd^{2+} ions were reduced to Pd (curve c). As expected, all above results show that the spherical Pd@Cys-C_{60} was successfully prepared.

Furthermore, electrochemical impedance spectroscopy (EIS) is used to evaluate the interfacial changes of the electrode. The semicircle diameter of impedance equals the electron transfer resistance (R_{et}), which controls the electron transfer kinetics of the redox probe at the electrode interface. Fig. 3A presents the impedance spectrum of the different stages. The Nyquist semicircle of Pd@Cys-C_{60}/GCE (curve b) in 2.5 mM $K_3Fe(CN)_6$/$K_4Fe(CN)_6$(1 : 1) containing 0.1 M KCl increased dramatically compared with the bare GCE (curve a), which indicates that Pd@Cys-C_{60} was immobilized on the GCE. In order to further verify the assembly process of the electrode, the assembly process was also monitored by cyclic voltammetry (CV) in the working solution (Fig. 3B). The conclusions of CV are confirmed with EIS.

The electrocatalytic activity of the Pd@Cys-C_{60} modified GCE toward glucose was investigated by CV. The CVs were recorded for the biosensor in PBS in the absence (a) and presence of 0.5 mM glucose (b) (Fig. 4). With the addition of glucose, the sensor triggers an electrocatalytic reaction, consequently, it changes the CV with an increase in the oxidation current and a concomitant decrease in reduction current, indicating that Pd@Cys-C_{60} has electrocatalytic activity for glucose oxidation.

The control experiments on the detection ability of the Nafion/Cys-C_{60}/GCE, Nafion/Pd^{2+}(Cys-C_{60})$_n$/GCE, and the Pd@Cys-C_{60}/GCE have been researched under the optimized experimental conditions (see Fig. S2, ESI†). It is seen that the Nafion/Cys-C_{60}/GCE and Nafion/Pd^{2+}(Cys-C_{60})$_n$/GCE only

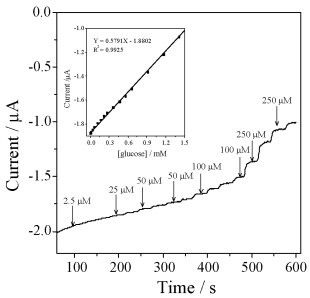

Fig. 5 Amperometric response of the biosensor to glucose under the optimized experimental conditions. Inset shows linear calibration curves.

display slight changes in current to additions of glucose. In contrast, the Pd@Cys-C_{60}/GCE exhibits appreciable increases in current, which may be attributed to the effect of Pd@Cys-C_{60} nanoparticles.

Fig. 5 shows the typical current–time dynamic response of the Pd@Cys-C_{60}/GCE towards glucose. The electrode responded quickly by the change of glucose concentration and reached about 95% of the steady-state current within 9 s. The amperometric signal shows a linear range from 2.5 μM to 1.0 mM with a correlation coefficient of 0.9925 and a low detection limit of 1.0 μM (S/N = 3). The analytical performances of the proposed biosensors are compared with previously reported nonenzymatic sensors (see Table S1, ESI†). As can be observed the proposed biosensor displays wider linear range, lower detection limit, and higher sensitivity.

To evaluate the effect of interferences (such as ascorbic acid, (AA), uric acid (UA), *p*-acetamidophenol (AP), and fructose) toward direct electrochemical oxidation of glucose, 0.1 mM AA, 0.1 mM UA, 0.1 mM AP and 0.1 mM fructose was added into 0.5 mM glucose solution and no observable interference on the current response of glucose was seen (signal change below 4.8%), respectively. The results (see Table S2, ESI†) showed that the glucose biosensor has good anti-interfering ability, which may be also attributed to the low working potential (−0.05 V) in the experiment.

The reproducibility and repeatability of the sensors were performed by six assaying electrodes prepared in the same condition. The relative standard deviation (R.S.D) was 4.1% in the presence of 0.5 mM glucose solution. The 5 successive measurements of a single sensor were tested in the presence of 0.5 mM glucose and revealed a R.S.D. of 3.9%. The stability of the glucose sensor was also investigated. The developed sensor was tested in the presence of 0.5 mM glucose solution each day, after 30 days, the response of the sensor decreased 7.6% compared to the initial response, which shows that the sensors have good stability.

To illustrate the feasibility of the biosensors in practical analysis, it is applied to detect glucose in human serum. The blood samples are 50-fold diluted with 0.1 M PBS (pH 7.4) before the measurements, and each sample is analyzed using a standard addition method with three times addition of a standard glucose solution. The corresponding results are given (see Table S3, ESI†). It can be seen that the biosensor gives good recoveries, indicating that the proposed electrode may have a potential for practical application.

In conclusion, spherical Pd@Cys-C_{60} nanoparticles *via* an *in situ* spontaneous reduction process have been successfully prepared. The results show that the Pd@Cys-C_{60} nanoparticles modified electrode exhibits good sensitivity, stability, and fast response for glucose. The spherical Pd@Cys-C_{60} nanoparticles may be a potential candidate as a catalyst support for electrochemical oxidation.

This work was supported by National Natural Science Foundation of China (21075100), the Ministry of Education of China (Project 708073), the Nature Science Foundation of Chongqing City (CSTC-2011BA7003 and CSTC-2009BA1003), State Key Laboratory of Electroanalytical Chemistry (SKLEAC 2010009) and specialized research fund for the doctoral program of higher education (20100182110015).

Notes and references

1 M. Feng, J. Zhao and H. Petek, *Science*, 2008, **320**, 359–362.
2 A. L. López, A. Mateo-Alonso and M. Prato, *J. Mater. Chem.*, 2011, **21**, 1305–1318.
3 H. W. Kroto, J. R. Heath, S. C. O'Brien, R. F. Curl and R. E. Smalley, *Nature*, 1985, **318**, 162–163.
4 C. Toumey, *Nat. Nanotechnol.*, 2010, **5**, 693–694.
5 M. Prato, *J. Mater. Chem.*, 1997, **7**, 1097–1109.
6 D. Bonifazi, O. Enger and F. Diederich, *Chem. Soc. Rev.*, 2007, **36**, 390–414.
7 Z. L. Wei, Z. J. Li, X. L. Sun, Y. J. Fang and J. K. Liu, *Biosens. Bioelectron.*, 2010, **25**, 1434–1438.
8 Y. Zhang, W. Liu, X. Gao, Y. L. Zhao, M. Zheng, F. F. Li and D. L. Ye, *Tetrahedron Lett.*, 2006, **47**, 8571–8574.
9 H. Wakai, T. Momoi, T. Shinno, T. Yamaudhi and N. Tsubokawa, *Mater. Chem. Phys.*, 2009, **118**, 142–147.
10 S. Q. Xiao, Y. J. Li, Y. L. Li, H. B. Liu, H. M. Li, J. P. Zhuang, Y. Liu, F. S. Lu, D. Q. Zhang and D. B. Zhu, *Tetrahedron Lett.*, 2004, **45**, 3975–3978.
11 V. Krishna, N. Noguchi, B. Koopman and B. Moudgil, *J. Colloid Interface Sci.*, 2006, **304**, 166–171.
12 H. Benyamini, A. Shulman-Peleg, H. J. Wolfson, B. Belgorodsky, L. Fadeev and M. Gozin, *Bioconjugate Chem.*, 2006, **17**, 378–386.
13 M. Plonska, K. Winkler, S. Gadde, F. D'Souza and A. L. Balchc, *Electroanalysis*, 2006, **18**, 841–848.
14 S. Y. Yang, G. X. Zhang, D. Q. Zhang, J. F. Xiang, G. Yang and D. B. Zhu, *Soft Matter*, 2011, **7**, 3592–3598.
15 D. M. Guldi, G. M. Aminur Rahman, V. Sgobba and C. Ehli, *Chem. Soc. Rev.*, 2006, **35**, 471–487.
16 H. W. Chang and J. S. Shih, *Sens. Actuators, B*, 2007, **121**, 522–529.
17 Z. Y. Bai, L. Yang, Y. M. Guo, Z. Zheng, C. G. Hu and P. Xu, *Chem. Commun.*, 2011, **47**, 1752–1754.
18 Y. J. Li, Z. H. Gan, N. Wang, X. R. He, Y. L. Li, S. Wang, H. B. Liu, Y. Araki, O. Ito and D. B. Zhu, *Tetrahedron*, 2006, **62**, 4285–4293.
19 T. R. Ohno, Y. Chen, S. E. Harvey, J. H. Weaver, R. E. Haufler and R. E. Smalley, *Phys. Rev. B: Condens. Matter*, 1991, **44**, 13747–13755.
20 G. H. Lee, J. H. Shim, H. Kang, K. M. Nam, H. Song and J. T. Park, *Chem. Commun.*, 2009, 5036–5038.
21 R. N. Goyal, V. K. Gupta and S. Chatterjee, *Biosens. Bioelectron.*, 2009, **24**, 1649–1654.
22 L. M. Lu, H. B. Li, F. L. Qu, X. B. Zhang, G. L. Shen and R. Q. Yu, *Biosens. Bioelectron.*, 2011, **26**, 3500–3504.
23 O. Stoilova, C. Jérôme, C. Detrembleur, A. Mouithys-Mickalad, N. Manolova, I. Rashkov and R. Jérôme, *Chem. Mater.*, 2006, **18**, 4917–4923.
24 Y. F. E, L. L. Bai, L. Z. Fan, M. Han, X. Y. Zhang and S. H. Yang, *J. Mater. Chem.*, 2011, **21**, 819–823.
25 J. D. S. Newman and G. J. Blanchard, *Langmuir*, 2006, **22**, 5882–5887.
26 A. Graja, I. Olejniczak, A. Bogucki, D. Bonifazi and F. Diederich, *Chem. Phys.*, 2004, **300**, 227–232.